Heliyon 10 (2024) e35122

Contents lists available at ScienceDirect

Heliyon

journal homepage: www.cell.com/heliyon

Research article

Synthesis and molecular structure exploration of novel piperidin-4-one imine derivatives combined with DFT and X-ray: A new class of antioxidant and anti-inflammatory agents

Rubina Siddiqui [a], Sana Shamim [b,*], Shamim Akhter [c], Samia Kausar [d], Sammer Yousuf [e], Ataf Ali Altaf [f], Zafar Saeed Saify [f], Fuad Ameen [g]

[a] Department of Pharmaceutical Chemistry, Faculty of Pharmacy and Pharmaceutical, Sciences, University of Karachi, Karachi, 75270, Pakistan
[b] Department of Pharmaceutical Chemistry, Dow College of Pharmacy, Faculty of Pharmaceutical Sciences, Dow University of Health Sciences, Ojha Campus, Karachi, Pakistan
[c] Department of Pharmaceutical Chemistry, Faculty of Pharmacy, Hamdard University Karachi, Pakistan
[d] Department of Chemistry, University of Gujrat, Gujrat, 50700, Pakistan
[e] H. E. J., Research Institute of Chemistry, International Center for Chemical and Biological Sciences, University, of Karachi, Karachi, 75270, Pakistan
[f] Department of Chemistry, University of Gujrat, Hafiz Hayat Campus, Gujrat, 50700, Pakistan
[g] Department of Botany and Microbiology, College of Science, King Saud University, Riyadh, 11451, Saudi Arabia

ARTICLE INFO

Keywords:
Piperidin-4-one
Imine derivatives
ADMET
Spectroscopy
XRD
DFT calculation
Antioxidant activity
Anti-inflammatory

ABSTRACT

Inflammation is one of the pertinent responses of the body, depending mainly on the process and factors involved in combating the oxidative species produced either by any infection or failure of the antioxidant pathways. In search of new compounds to exhibit antioxidant and anti-inflammatory activity here, we have successfully reported the synthesis of three novel compounds of Piperidin-4-one skeleton by adopting simple and convenient methods. Compound **1**, (3, 3-dimethyl-2, 6-bis(3,4,5-trimethoxyphenyl) piperidin-4-one) was synthesized by one-pot Mannich condensation reaction having good yield (88 %). Furthermore in the next step highly functionalized imine derivatives, Compound **2** (3,3-dimethyl-2,6-bis (3,4,5-trimethoxyphenyl) piperidine-4-one) hydrazine carbothioamide) and Compound **3** (3,3-dimethyl-2,6-bis(3,4,5-trimethoxyphenyl) piperidin-4-one oxime) were prepared by the condensation reaction with thiosemicarbazide and hydroxylamine hydrochloride with compound **1**, respectively. The structure of the compounds has been deduced by the combined use of modern spectroscopic and single crystal x-ray diffraction (XRD) techniques. *in-silico* ADMET studies predict pharmacokinetic properties and showed that compounds are non toxic on vital organs. The optimized geometry and reactivity parameters of compounds were further calculated based on the B3LYP/6-31G (d, p) density functional theory (DFT). The negative values of chemical potential follow the trend as **2** (−0.2101) > **3** (−0.2198) > **1**(-0.2233) signifies that all compounds are reactive in nature as evident from *in-vitro* antioxidant and anti-inflammatory response were determined by using the DDPH assay and protein denaturation methods respectively. Compounds possess good radical scavenging activity having IC 50 values 30.392 μM (**2**), 37.802 (**1**) μM, and 72.285 (**3**) μM, and anti-inflammatory response in same manner indicating that **2** (71.3 %) is more active than

* Corresponding author.
E-mail address: sana.shamim@duhs.edu.pk (S. Shamim).

https://doi.org/10.1016/j.heliyon.2024.e35122
Received 25 January 2024; Received in revised form 23 July 2024; Accepted 23 July 2024
Available online 25 July 2024

compound **1** (43.5 %) and **3** (39.3 %) marking them as a potential antioxidant and anti-inflammatory agents.

1. Introduction

Oxygen utilization is essential for the survival and functioning of normal catabolic and physiological processes, as a key mediator of the intracellular signaling cascade. As a major component of the Reactive Oxygen species (ROS) system like hydroxyl (OH), Superoxide anions (O^{2-}), and Nitric oxide (NO), an efficient protection system [1]. Any disruptions in this system are the causative factor of oxidative stress leading to cell function loss, apoptosis, or necrosis leading to the altered biochemical process causing various diseases like cancer, cardiovascular diseases, aging, diabetes, inflammation, nephrotoxicity, liver cirrhosis, etc. Therefore, the compounds that prevent the propagation and onset of oxidative stress are of prime importance in preventing these disease conditions [2].

Heterocyclic piperidine ring, an important pharmacophore of numerous natural alkaloids has diverse pharmacological properties including anti-cancer, anti-histamine, bactericidal, fungicidal, insecticidal, stimulant, and depressant of the central nervous system [3–6]. Among the derivatives of piperidine, piperidin-4-one (4-piperidone) is commonly used as an intermediate or a starting reagent to synthesize various biologically important compounds such as antihistamine (dorastine), anticholinergic (propiverine), synthetic opioid (fentanyl), antipsychotic (osanetant, pimozide) [7,8], and many more. Similarly, 2, 6-diphenylpiperidin-4-one derivatives are reported to have anti-cancer, anti-inflammatory, anti-microbial, local anesthetic, and analgesic properties [9–11].

One of the key reactant used in synthesis is 3, 4, 5-trimethoxybenzaldehyde(TMB), commonly used in the synthesis of antibacterial (trimethoprim) and antioxidant agents (isoamoenylin), it stimulates the hydrolysis of tubulin-dependent GPT and stops the unfolding of tubulin [12,13]. Structure activity relationship showed that 3, 4, 5-trimethoxy phenyl substitution is critical for antiproliferative activity, among different derivatives of piperidine [14]. Benzoyl hydrazones of 2,6-diphenylpiperidin-4-one also exhibit antioxidant, anticholinesterase, and anticancer activities [15]. Currently, biocatalytic synthesis of piperidine derivatives is reported in good yield through an immobilized lipase-catalyzed, multicomponent one-pot reaction. Various substituted piperidines, piperidones, and spiropiperidines play an important role in pharmaceutical engineering [16,17].

Structurally, the presence of two important functionalities (carbonyl and amine) of piperidin-4-one allows this molecule to be introduced with a range of substituents that result in an important class of compounds including carbazide, thiosemicarbazide, oxime,

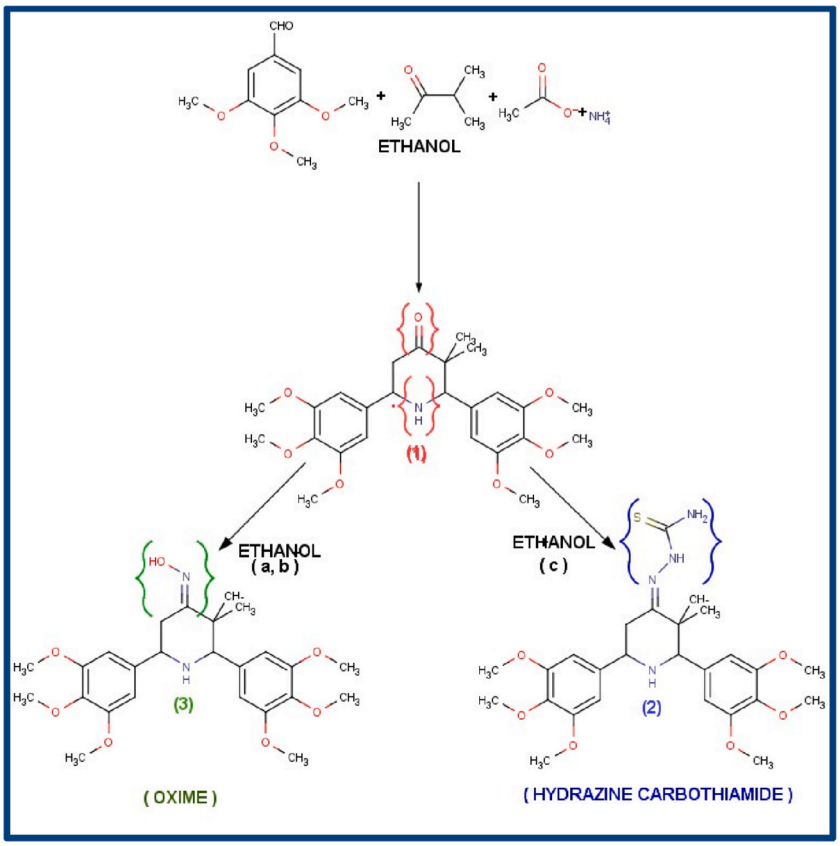

Scheme 1. Synthesis of compounds **1**, **2,** and **3**. Where; **a**: Hydroxylamine HCl**, b**: Sodium acetate trihydrate, and **c**: thiosemicarbazide.

oxime-ether, thiazolidones, oxirane, thiazole, and triazine [18–21] Its hydrazones and oximes serve as important ligands to form coordination complexes as the presence of electronegative nitrogen, sulphur, and oxygen increases the coordination potential [22]. In light of these studies, new imine derivatives of 2, 6-diphenylpiperidin-4-one were synthesized, followed by characterization based on molecular spectroscopic technique following DFT calculation to explore energetic behavior and stability of synthesized compounds having enough potential to interact with macromolecules. DFT calculations are an indispensable tool in the field of computational chemistry and drug design, providing essential insights that bridge the gap between theoretical predictions and experimental observations. The radical scavenging response of compounds was assayed by using DPPH and *in-vitro* anti-inflammatory activity was also determined.

2. Experimental

2.1. Materials, physical measurements

Solvents, reagents, and DPPH used for synthesis and analysis were purchased from Merck and TCI Japan and used without any additional purification. The melting points of compounds were recorded on Buchi 434 instrument. Ultraviolet spectra were monitored by using a Shimadzu UV-1600 spectrophotometer. MAT112 and JEOL mass spectrometer (JMS) were used to find out the molecular mass and fragmentation pattern of synthesized compounds. The presence of imine functionality was further confirmed by considering the change in the position of peaks in IR spectra monitored by making KBr disc mounted in Jasco 302 Fourier transformed infrared (FTIR) spectrophotometer. Using tetramethylsilane (TMS) as an internal standard and chloroform as solvent, ^{1}H NMR spectra were recorded on Bruker AM 300 and 400 MHz spectrophotometers.

2.1.1. Synthesis and Spectral analysis of 3, 3-dimethyl-2, 6-bis (3, 4, 5-tri-methoxyphenyl) piperidin-4-one (1)

Compound **1** was synthesized by following the protocol as described by Baliah et al. [23] The mixture of 3, 4, 5-tri methoxy benzaldehyde (3.92 g, 0.2 mol), methyl isopropyl ketone (1.5 mL, 0.1 mol) and dried ammonium acetate (0.77 g, 0.1 mol) refluxed in ethanol (50 mL). Reaction completion was monitored through TLC. Concentrated hydrochloric acid (5 mL) was added upon completion of the reaction. The acidic precipitates were separated, washed, and suspended in acetone and then allow to neutralize by adding aqueous ammonia. After washing with cold water, obtained precipitates were vacuum dried and recrystallized from absolute ethanol (Scheme-1).

Compound **1**: yield; 88.3 %, Colorless crystals, M.P; 166 ± 1 °C, M.W; 459.53, UV $_\lambda$ max nm (Methanol); 213, 229 and 268. IR $_\upsilon$ max (KBr) cm^{-1}; 3460, 3307, 2949, 1697, 1593, 1330, 1130, 914 and 837. EIMS *m/z* (%-abundance); 459.3 M$^+$ (39), 388(22.7), 374.3 (31.3), 264(21.7), 236(15.23), 222.2(36.93), 194.1(100), 179.1(51.93), 91(18.66). ^{1}H NMR ($CDCl_3$, 400 MHz) δ (ppm); 6.68 (s, 2H, arom. H), 6.64 (s, 2H, arom. H), 3.959 (s, 12H, –OCH_3), 3.697 (s, 6H, -OCH3), 2.88 (t, J = 12.8Hz,1H, piperidinyl H), 2.455 (d, J = 13.2 Hz, 1H, piperidinyl H), 1.984 (s,1H(ax), CH_2), 1.594 (s,1H (eq), CH_2), 1.208 (s, 3H, CH_3), 0.963 (s,3H, CH_3).

2.1.2. Synthesis and Spectral analysis of (Z)-2-(3, 3-dimethyl-2, 6-bis (3,4,5-tri-methoxyphenyl) piperidine-4-one hydrazine carbothiamide (2)

In absolute ethanol (50 mL) mixture of compound 1 (0.45g, 0.01 mol) and thiosemicarbazide (0.091 g, 0.01 mol) was refluxed with continuous stirring on the hot plate. After 3 h of reaction, the content was poured in ice cold water to obtain a precipitate of product washed again with cold water and finally crystallized from ethanol (scheme-1).

Compound **2**: yield; 82 %, Light yellow crystals, M.P; 203 ± 1 °C, M.W; 532.65, UV $_\lambda$ max nm (Methanol); 207, 273. IR $_\upsilon$ max (KBr) cm^{-1}; 3466, 2933, 2372, 2054, 1639, 1593, 1328 and 839. EIMS *m/z* (%-abundance); 532.2 M$^+$ (25), 456(19.2), 441(11.5), 415(11.9), 374(100), 277(16.6), 262(42.9), 220(95.4), 196(49.6), 154.1(12.2). ^{1}H NMR ($CDCl_3$, 400 MHz) δ (ppm); 10.419 (s, 1H, NH), 8.336 (s, 2H, NH_2), 7.240 (s, 1H, NH-piperidine), 6.46 (s, 2H, arom. H), 6.41 (s, 2H, arom. H), 3.830 (s,12H, –OCH_3), 3.769 (s, 6H, –OCH_3), 3.17 (t, J = 14Hz, 1H, piperidinyl H), 2.65 (d, J = 15 Hz, 1H, piperidinyl H), 2.882 (s, 1H(ax), CH_2), 2.303 (s, 1H (eq), CH_2), 0.986 (s,3H, CH_3), 0.886 (s,3H, CH_3).

2.1.3. Synthesis and Spectral analysis of 3, 3-dimethyl-2, 6-bis (3, 4, 5-tri-methoxyphenyl) piperidin-4-one hydrazine oxime (3)

In absolute ethanol (50 mL) mixture of 1 (0.45 g, 0.01mol) and thiosemicarbazide (0.091 g, 0.01 mol) refluxed with continuous stirring on hot plate. After 3 h of reaction, the content was poured in ice cold water and obtained precipitate of product washed with cold water and recrystallized from ethanol (scheme-1).

Compound **3**: yield; 76 %. Colorless powder. M.P; 174 ± 1 °C. M.W; 474.55, UV $_\lambda$ max nm (Methanol); 207, 255 and 268. IR $_\upsilon$ max (KBr) cm^{-1}; 3460, 2933, 2835, 1597, 1379 and 923. EIMS *m/z* (%-abundance); 474.4 M$^+$ (29), 457(6.6), 374(10.4), 264.2(10), 196 (100), 169(6). ^{1}H NMR ($CDCl_3$, 400 MHz) δ (ppm); 7.771 (s, 1H, NH), 6.72 (s, 2H, arom.H), 6.64 (s, 2H, arom. H), 3.885 (m, 1H, piperidinyl H), 3.718 (s, 12H, –OCH_3), 3.688 (s, 6H, –OCH_3), 3.612 (s, 1H, piperidinyl H), 1.287(d, J = 10.4Hz,IH, CH_2), 1.206 (m, 1H, CH_2), 1.151 (s, 3H, CH_3), 1.028 (s, 3H, CH_3).

2.2. XRD-data collection and elucidation

Bruker SMARTAPEX-11diffractometer, attached to CCD detector is used to collect diffraction data of compounds **C1** and **C2**. Computed data were resolved by Bruker SAINT program using WinGX, incorporated with SHELXTL program scheme. ORTEP-3 program is used to present the molecular structure of crystal in ORPT (Oak Rigid Thermal Ellipsoid Plot) view, whereas the

interactions were construed with PLATON and visualized by MERCURY3.6 software [24–27].

2.3. DFT-computational details

DFT-B3LYP/6-31G (d, g) density functional theory has been used to compute the electronic properties of compounds [28]. The ground states geometries of compounds (**1–3**) were optimized through hybrid functional B3LYP and basis set 631G (d, p) [29], whereas Frontier Molecular Orbitals (FMOs) were analyzed to find out the energy gaps and to calculate reactivity parameters of the optimized compounds. Mullikens Atomic Charges (MAC) and molecular electrostatic potential (MEP) were calculated for the elucidation of charge distribution on the structure and reactivity of these compounds for biological targets.

2.4. In-silico ADMET properties

The *in-silico* ADMET properties of these newly synthesized compounds is studied by using the swiss ADME webserver (http://www.swissadme.ch) [30] and Protox-II webserver [31].

2.4.1. DPPH radical scavenging activity

The radical scavenging activity of any compound is a determinant of its possible pharmacological responses. DPPH assay method is the most common and effective assay method in determining antioxidant activity [32]. Here, we use 1 ml of 0.1 mM of DPPH (ethanol) in 2 ml of concentrations 100, 50, 25, 10, 5, and 2.5 μg/ml of compounds **1–3** in a triplicate manner. To avoid the interference of light, solutions were kept in the dark for 30 min. Ascorbic acid (2:1) is used as standard, DPPH as control, and samples were observed at wavelength 517 nm using UV–Vis spectrophotometer. % DPPH inhibition activity was calculated using the formula:

$$\text{Inhibition ratio (\%)} = (A_s - Ac)\ /A_s \times 100$$

Where, A_s is the absorbance of the standard and A_C is the absorbance of the compound solution (**1–3**) of variable concentration. IC_{50} was calculated by using values from a linear regression graph.

2.5. In-vitro anti-inflammatory activity

The In-vitro anti-inflammatory response of the synthesized compounds was determined by the protein denaturation method [33]. The percent inhibition of compounds **1–3** (n = 3) was analyzed at concentrations 100, 50, 25, 10, 5, and 2.5 μg/ml and compared with standard (Diclofenac Na 100 μg/ml). Egg albumin solution (1 ml of 1 mM) was attenuated with standard and control (distilled water), at each concentrations in individual test tubes incubating it for 15 min at 27±1 °C followed by incubating in the water bath at 70 °C for 10 min, samples were scan at a wavelength of 660 nm. The percentage denaturation inhibition was calculated by applying the formula:

$$\text{Percentage Inhibition (\%)} = (A_s - Ac)\ /A_s \times 100$$

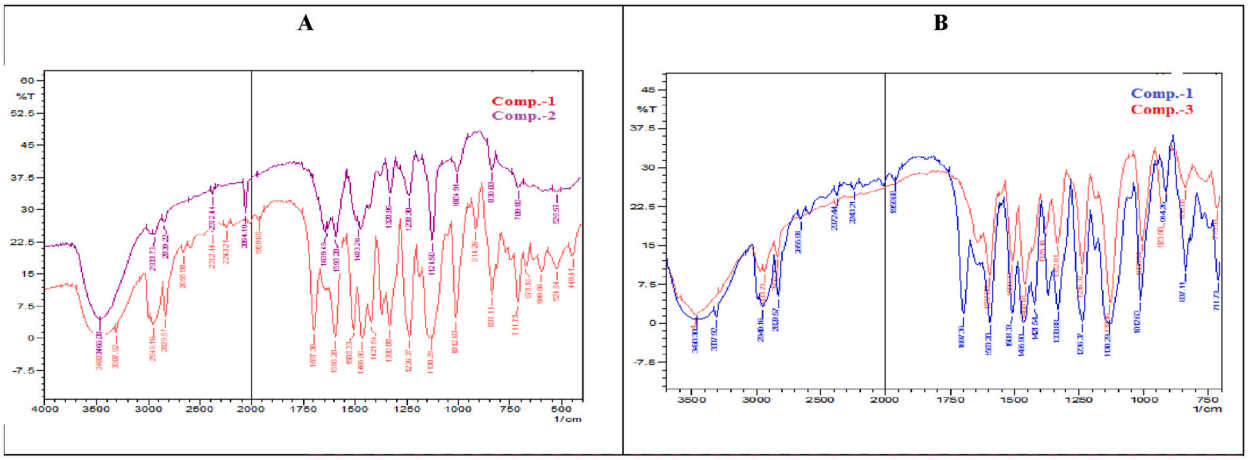

Fig. 1. A & B. Comparative FT-IR-spectra of compound **2** and **3** with parent compound **1**.

3. Results and discussion

3.1. Synthesis

A one-pot synthesis is a useful approach for designing and developing of new complex molecules from simple reagents. In the present study a new heterocyclic compound 3,3-dimethyl-2,6-bis (3,4,5-tri-methoxyphenyl) piperidin-4-one (**1**) was synthesized by mannich condensation reaction among 3,4,5-trimethoxybenzaldehyde, methyl isopropyl ketone and ammonium acetate yielding 88 % of the compound, from which highly functionalized imine derivative compound **2** was successfully obtained by nucleophilic addition reaction of nitrogen of thiosemicarbazide with the carbonyl group of compound **1** in acidic medium with elimination of water molecule. Compound **3**, an oxime derivative obtained by condensation reaction between compound **1** and hydroxylamine hydrochloride (Scheme-1). The synthesis of compounds (**1–3**) was monitored by the TLC sytem comprised of ethyl acetate and hexane (3:7), same system was used to purify the compounds (**1–3**) exhibiting good yields, followed by spectroscopic characterization using UV–Visible, FT-IR, ^{1}HNMR, Mass spectroscopy and X-ray crystallography.

3.2. FT-IR, ^{1}HNMR, and mass spectra of compounds

The FT-IR spectrum of compound **1** revealed stretching bands at 3460, 2949, 1697, and 837 cm^{-1} for secondary amine (N–H), sp^3 C–H, carbonyl (C=O), and sp^2 (aromatic) respectively [25]. Disappearance of the absorption band of carbonyl (1697) and appearance of the C=N band at 1639 cm^{-1} and the presence of a stretching bond around 3466 cm^{-1}(NH_2) confirmed the synthesis of thiosemicarbazone derivative compound **2** (Fig. 1 A &B). Similarly, the presence of 3460 (N–OH) and 1379 cm^{-1} (C=N) stretching bonds indicates the presence of the oxime function group in compound **3** (Fig. 1). The ^{1}H NMR spectrum showed characteristic singlets at δ 10.419 and δ 8.336 of corresponding NH and NH_2 groups of hydrazine respectively. A multiplet at δ 6.682 - δ 6.408 appeared due to the aromatic proton further supporting the structure of synthesized compounds. While the aliphatic methyl of the 4-piperidone ring appeared as δ 0.82 and δ 1.03 respectively. Molecular mass was confirmed by corresponding *m/z* peaks of compounds (459, 532, and 474) in mass spectra which is in accordance with the projected molecular formula of the respective compounds (supplementary material).

3.3. X-ray crystallography

The sythesis method yielded fine crystals of compounds **1** and **2** in the triclinic system, with space group *P–I* and unit cells of compounds containing two independent molecules (Fig. 2a and b). The crystal structures are reported in the CCDC as RA2 (2178085) for compound **1** and RA2r (2178084) for compound **2**. The parent compound **1** contains a central cyclohexane ring, A (C-7—C-11/N-1), with an equatorial oriented dimethyl group at C-8, and two planar tri-methoxy rings (B and C) at C-7 and C-11. Piperidine ring adopts a chair conformation. Structurally **2** was found to be similar to **1** with the difference in the presence of the hydrazine carbothioamide group (S-1/N-2-N-4/C-23) in place of the carbonyl functional group. Crystallographic data of compounds given are in Tables 1 and **2**, Table 3 (supplementary material)

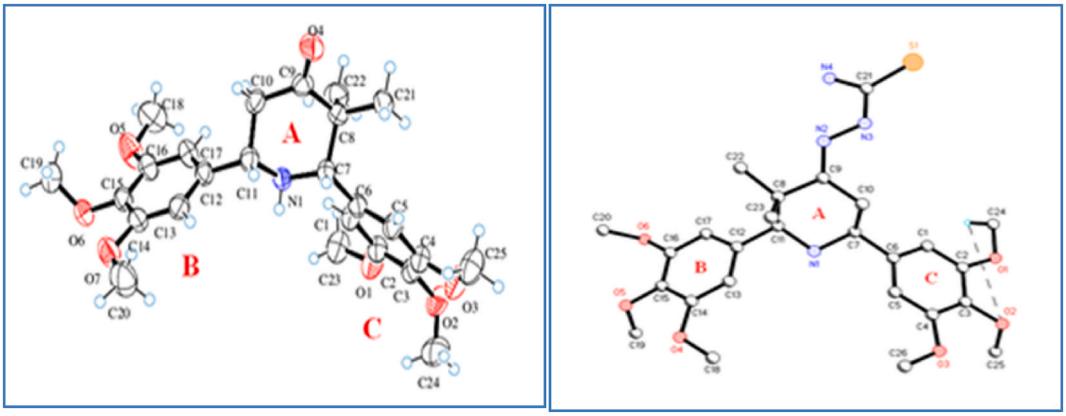

Fig. 2. (a). The molecular structure of parent compound **1** shows the numbering of atoms. All non-H atoms are presented by 50 % probability displacement ellipsoids. (b) Compounds **2**, also showed compound **1** and **2** also stabilized via C-24—H-24C···O-2. (dash line represent the intermolecular interactions).

Table 1
Crystal data and structure refinement for compounds **1** and **2**.

Compounds	1	2
Empirical formula	$C_{50}H_{66}N2O_{14}$	$C_{26}H_{36}N_4O_6S$
Formula weight	919.05	532.65
Temperature	273(2) K	100(2) K
Wavelength	0.71073 Å	1.54178 Å
Crystal system	Triclinic	Triclinic
Space group	*P-1*	*P-1*
Unit cell dimensions	**a** = 9.2021(5) Å **b** = 12.9290(7) Å **c** = 20.7220(11) Å α = 82.6570(10)° β = 80.4410(10)° γ = 83.2270(10)°	**a** = 82.6570 (10) Å **b** = 80.4410 (10) Å **c** = 11.7423 (16) Å α = 84.343 (6)°. β = 72.576 (6)°. γ = 80.526 (6)°.
Volume	2399.4(2) $Å^3$	1356.4(3)$Å^3$
Z	2	2
Density (calculated)	1.272 Mg/m^3	1.304 Mg/m^3
Absorption coefficient	0.093 mm^{-1}	1.452 mm^{-1}
F(000)	984	568
Crystal size	0.44 x 0.44 × 0.20 mm	0.260 x 0.200 × 0.080 mm
Theta range for data collection	1.00 to 25.50	3.951–44.668°.
Index ranges	−11 ≤ h<=11, −15 ≤ k<=15, −25 = l ≤ 25	−9 ≤ h<=9, −10 ≤ k<=10, −10 ≤ l<=10
Reflections collected	2	6694
Independent reflections	8931 [R_{int} = 0.0197]	2105 [R_{int} = 0.0430]
Completeness to theta = 67.679°	100.0 %	97.5 %
Refinement method	Full-matrix least-squares on F^2	Full-matrix least-squares on F^2
Data/restraints/parameters	8931/0/603	2105/0/299
Goodness-of-fit on F^2	1.028	1.059
Final R indices [I > 2sigma(I)]	R_1 = 0.0432, wR_2 = 0.1260	R_1 = 0.0486, wR_2 = 0.1126
R indices (all data)	R_1 = 0.0822, wR_2 = 0.1639	R_1 = 0.0623, wR_2 = 0.1194
Largest diff. peak and hole	0.193 and −0.180 e.$Å^{-3}$	0.314 and −0.240 e.$Å^{-3}$

Table 2
Hydrogen bonds geometry (Å, °) of compounds **1** and **2**.

D—H…A	D—H/Å	H…A/Å	D…A/Å	D—H…A/°
Compound 1				
N-1—H-1A…O-9	0.82(3)	2.34(3)	3.162(4)	177(3)
N-2—H-2A…O-6	0.94(4)	2.23(4)	3.161(4)	175(3)
Compound 2				
N-3—H-3A…O-4i	0.81(5)	2.38(4)	3.178(6)	173 (4)
N-4—H-4B···S-1ii	0.83	2.59	3.381	161 (4)
C-26—H-26B···O-2iii	0.98	2.56	3.449(6)	151
C-24—H-24C···O-2 iv	0.98	2.35	2.987(6)	122

Symmetry Code: (i) -x, -y, -z, (ii) 1-x, -y, 1-z, (iii) 2-x, 1-y, 1-z, (iv) -x, 1-y, -z.

Table 3
B3LYP/6-31G (d, p) computed values of ELUMO, EHOMO, and EHOMO-ELUMO gap (ΔE) of compounds **1**–**3**.

Compounds	ELUMO (Hartree)	EHOMO (Hartree)	EHOMO-ELUMO gap ΔE (Hartree)
1	−0.15653	−0.29010	0.134
2	−0.15151	−0.26864	0.117
3	−0.14740	−0.29219	0.145

3.4. Crystal packing of compounds 1 and 2

Neighboring molecules in the crystal lattice of compound **1** are linked with each other via N-1—H-1A… O-9 and N-2—H-2A…O-6. Compound **2** was found to exhibit the intramolecular (C-24—H-24C···O-2) hydrogen bond, to form S6 group set (Fig. 3). As well as, in the crystal lattice of **2**, molecules were also found to be connected with each other via N-4—H-4B···S-1 intermolecular interactions to form R_2^2 (8) ring motifs (Fig. 4). The crystal packing further stabilized via N-4—H-3A…O-4 and C-26—H-26B···O-2 intermolecular interactions. Details regarding the crystal structure of the compounds are given in supplementary material.

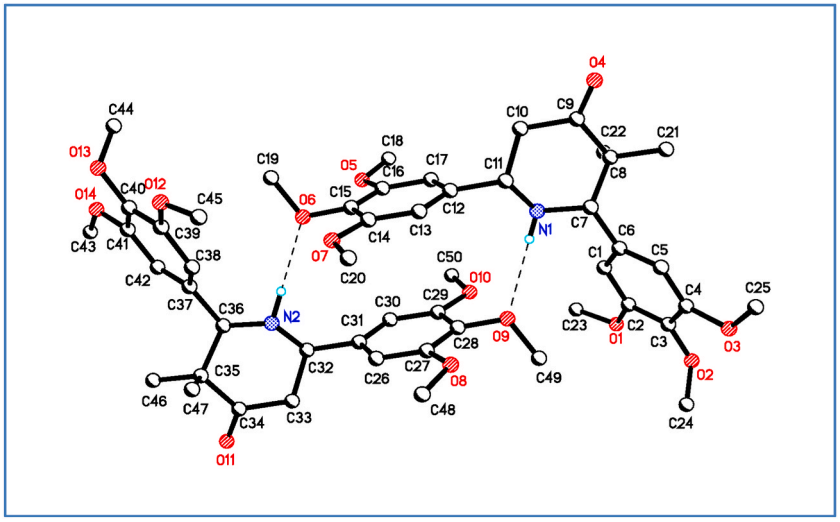

Fig. 3. The molecules of compound **1** linked by N-1—H-1A…O-9 and N-2—H-2A…O-6 interactions.

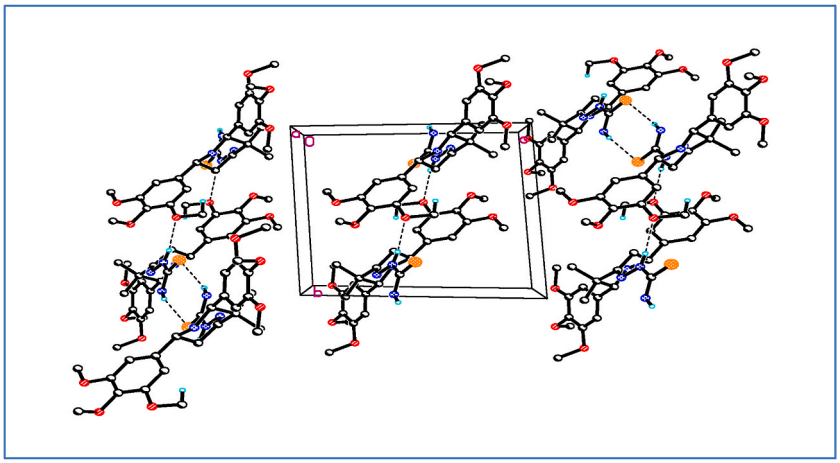

Fig. 4. R22 (8) ring motifs are formed among molecules through the contribution of N-4—H-4B…S-1 intermolecular hydrogen bonds.

3.5. DFT calculations (quantum chemical computational studies)

The electronic properties predicted by DFT aids in identifying the most reactive and stable structures, which is essential for the synthesis and practical application of new compounds, also predict the binding affinities with biological targets, enhancing the understanding of binding mechanisms.

3.6. Frontier Molecular Orbitals (FMOs) and chemical reactivity descriptors

The FMO Stability and reactivity characteristics of the compounds were investigated by finding the energy gap between an electron donor (HOMO) and acceptor (LUMO) orbitals. This alteration in energy band gap due to different functional groups causes the diverse chemical reactivity patterns among the compounds with favorable characteristics that can be defined structurally.

The FMO and chemical reactivity of compounds **1–3** were calculated at B3LYP/6-31G (d, p) basis set (Fig. 5). The stability and reactivity characters of compounds were investigated by the energy gap between an electron donor (HOMO) and acceptor (LUMO) orbitals. This alteration in energy band gap due to different functional groups causes diverse chemical reactivity patterns among the compounds with favorable characteristics that can be defined structurally [34]. Computed values of E_{LUMO}, E_{HOMO} and E_{HOMO}-E_{LUMO} gap (ΔE) and chemical reactivity descriptors of optimized structures enlisted in Tables 3 and 4 respectively.

From the computed values the most thermally and kinetically stable was found to be compound **3** whereas **2** was found to be the most attracted towards charge from the environment. Negative values of chemical potential follow the trend as **2** (−0.2101) > **3** (0.2198) > **1**(−0.2233) which reveal that compound have a greater capability of charge transfer and all compounds are reactive in

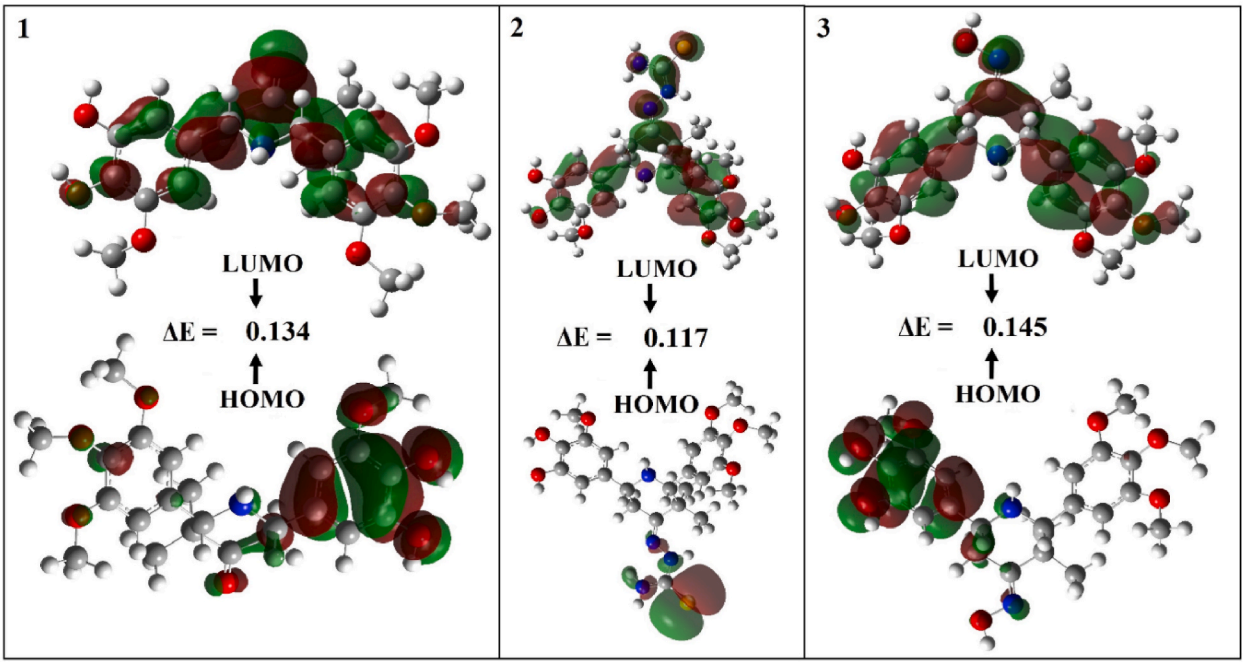

Fig. 5. Computed Frontier Molecular Orbitals (FMOs) values (ΔE) of compounds 1–3.

Table 4
B3LYP/6-31G (d, p) computed chemical reactivity parameters of compounds **1**–**3**.

Compounds	Electron Affinity (EA)	Ionization Potential (IP)	Electro-negativity (χ)	Electro -philicity (ω)	Chemical Potential (μ)	Global Hardness (η)	Global Softness (σ)
1	0.1565	0.2901	0.2234	0.3734	−0.2233	0.06679	7.4867
2	0.1515	0.2686	0.2101	0.3768	−0.2101	0.05857	8.5375
3	0.1474	0.2922	0.2197	0.3337	−0.2198	0.07239	6.9066

nature predicting them as potential biological candidates.

3.7. Molecular electrostatic potential (MEP) analysis

Molecular electrostatic potential (MEP) indicates the magnitude of charge (negative and positive regions) in 3D way along with the shape and size [35] All blue-colored hydrogen atoms in Fig. 6, suggested the comparative nonappearance of the electron around hydrogen atoms whereas the electronegative atoms such as oxygen (O) and nitrogen (N) having red color indicates the more strength of electron density that showed a preferred site for electrophilic attack.

3.8. Mulliken atomic charges (MAC) analysis

Information obtained from molecular orbital has been applied in computing Mullikens atomic charges which are used to understand and relate molecular properties to their structures. These charge distribution analyses give information about the polarizability, dipole moment, and electronic structure of any compound, and hence reactivity of these compounds for biological targets can be evaluated [36]. Calculated distribution of charges on compounds (Fig. 7) indicated the presence of highly electronegative atoms like oxygen (O) and nitrogen (N), showed by orange to reddish color and green color in the figure showed the distribution of positive charges on carbon and hydrogen atoms in compounds.

Compounds (**1–3**) exhibits tendency to react whereas compound **2** have shown maximum softness values and lesser energy gaps allowing for the highest number of charge transitions which signifying its reactive nature which defines its reactive nature as compared to other compounds and potential for biliological activities.

3.9. In-silico ADMET properties

The Absorption, distribution, metabolism, excretion and toxicity (ADMET properties) of any molecule plays an important role in determining its importance as a future drug. These parameters were studied by using Swiss ADME and protox-2 free webservers. The

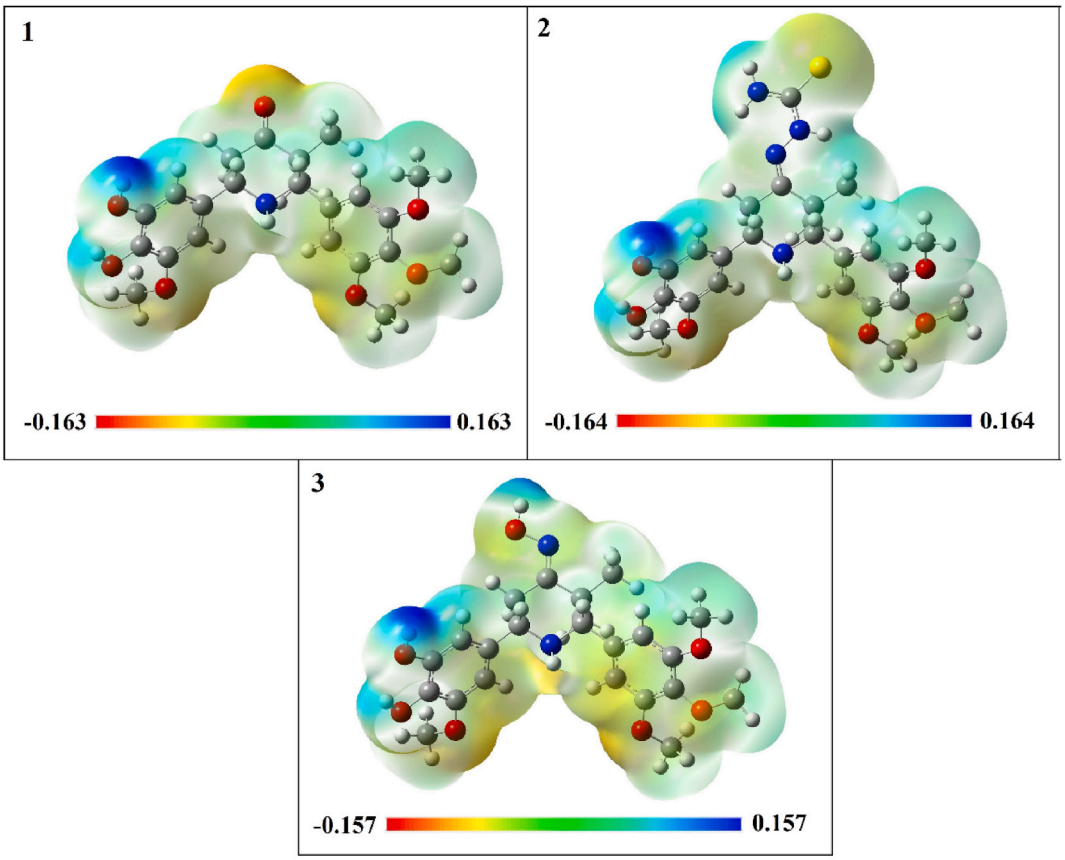

Fig. 6. Calculated molecular electrostatic potential (MEP) of the compounds **1–3.**

predicted results are shown in Table 5, indicating that all the compounds synthesized obeys the Lipinski's rule of five, exhibiting good drug likeness properties hence can be potentially used as drug agents.

The predicted activity of the compounds (**1–3**) against the cytochrome P450 isoforms was also studied and found that all the compounds are active against the Cytochrome P2D6, which is involved in the serotonin reuptake [37,38]. In other words these compounds might exhibit their role as SSRI (selective serotonin reuptake inhibitors). Their toxicity parameters were also studied by in-silico approach and found that they can cause respiratory, immuno and nephrotoxicity, at 550, 500 and 75 mg/kg of Compound **1**, **2** and **3**, respectively which needs to be assured by the in-vivo studies as all the compounds can cross the blood brain barrier (BBB).

This computational data indicates that these compounds qualified for further in vitro and in vivo development studies and have the potential to be a drug agents**.**

3.10. DPPH radical scavenging activity

The ability of a compound to trap free radicals is a determinant of its radical scavenging activity. The scavenging effects of compounds **1**, **2,** and **3** were expressed as a percentage of radical inhibition, % DPPH. Compound **2** exhibits the highest activity against compounds **1** and **3**. The IC_{50} values of compounds **2**, **1,** and **3** are 30.392 μg/ml, 37.802 μg/ml, and 72.857 μg/ml, respectively calculated by using an online tool (IC 50 Calculator) [39] pointing to the strong antiradical activity of compound **2** in comparison with the parent(**1**) and other analogue(**3**) but not as good in comparision to the standard ascorbic acid having IC_{50} 22.23 μg/ml (Table 6).

Structure-activity study showed that Compound **2** has reactive functionalities including primary and secondary amines containing nonbonding electrons that may produce antioxidant properties due to electron-donating groups similarly compound **1** showed antioxidant potential due to the presence of carbonyl group that becomes activated by donating its lone pair electrons. Oxime shows less activity as the electrophilicity of imino carbon is lower in oximes. All the synthesized compounds (**1–3**) showed antioxidant potential due to the presence of methoxy substituents [40].

3.11. In-vitro anti-inflammatory activity

The in vitro anti-inflammatory efficiency of compounds (**1–3**) was calculated in comparison with the standard (diclofenac sodium) through the protein denaturation method (mean ± SD). The protein denaturation potency of compounds **1, 2**, and **3** was expressed in

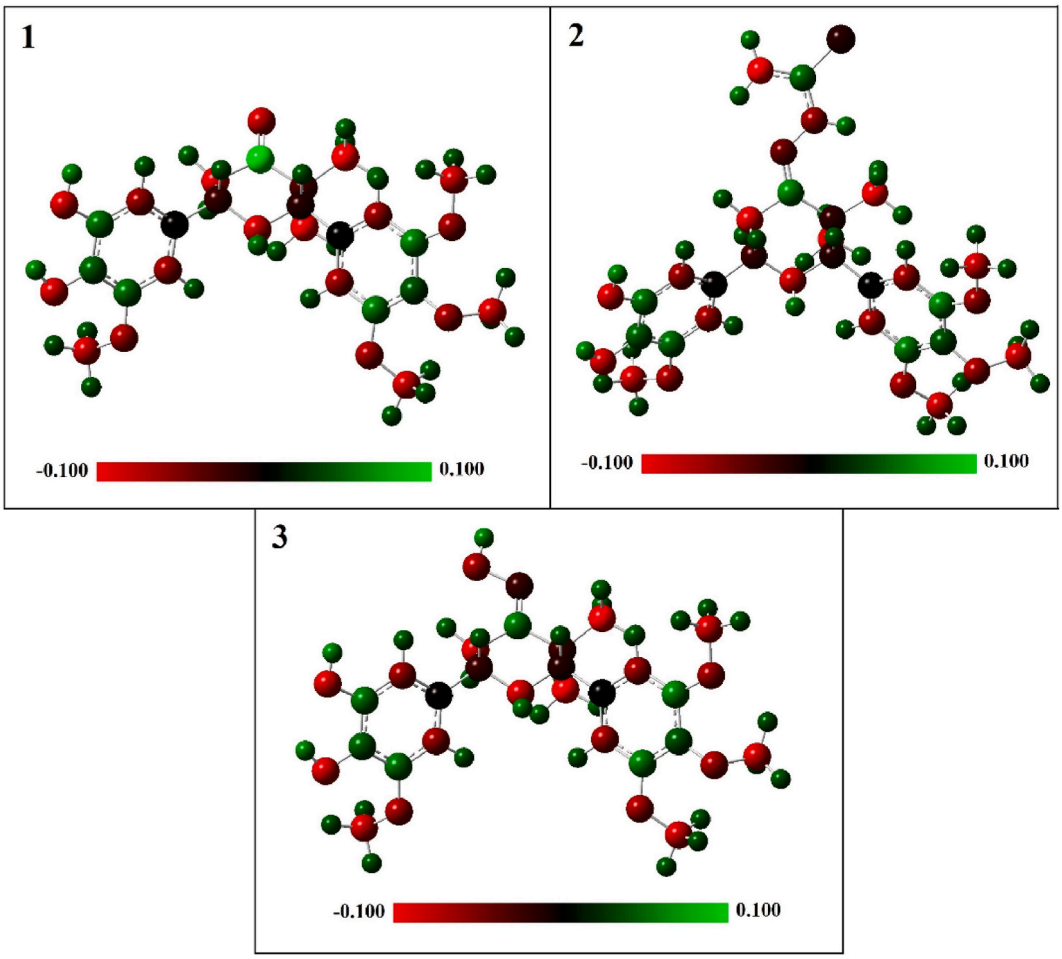

Fig. 7. DFT-B3LYP/631g (d, p) calculated Mullikens Atomic Charges (MAC) of the Compounds **1**–**3**.

percentage in a triplicate manner. These results assure that compound **2 (**71.3 %) is more active than compound **1** (43.5 %) and 3 (39.3 %) (Table 7) but not as effective as standard (diclofenac sodium)marking it as a potential antioxidant and anti-inflammatory agent among the synthesized compounds.

4. Conclusion

In this study by using small molecules, highly functionalized novel imine derivatives (compounds **2** and **3**) were successfully synthesized by an easy route. The developed synthetic method yields fine crystals of compounds **1** and **2** in the triclinic system. DFT studies explores the energetic behavior, stability, and reactivity of synthesized compounds with macromolecules by computing their thermal and kinetic stability. Negative values of chemical potential follow the trend as **2** (−0.2101) > **3** (0.2198) > **1**(−0.2233) which reveals that these compounds have a greater capability of charge transfer and all compounds are reactive in nature due to the presence of methoxy, amine and sulphur substituents. The negative values also showed that compounds are stable, along side showacsing good values against all pharmacokinetic parameters predicted through swissADME, revealing that compounds posses drug-like properties. Compound **2(**Z-2-(3, 3-dimethyl-2, 6-bis (3,4,5-tri-methoxyphenyl) piperidine-4-one hydrazine carbothiamide) showed significant antioxidant and anti-inflammatory potential among all compounds. Therefore, herein we can conclude that slight modification in structure may affect the reactivity and potency of the compound, confirmed by the DFT calculation and biological studies. Compound **2** having a thiazide group is more reactive, potent and might be used in future for the development of new chemical entity as anti-inflammatory agents.

Supplementary Information Supplementary information (H^1NMR and Mass Spectra, and Table, containing the bond lengths and bond angles for compounds **1** and **2** (crystallography).

Table 5
In-silico predicted ADMET properties of compounds **1**–**3**.

Compound	MW	NHA	NAHA	NRB	NHBA	NHBD	TPSA	Log P	Solubility (mg/ml)	Lipinski violations
1	459.53	33	12	8	8	1	84.48	3.16	1.99E-02	0
2	532.65	37	12	10	8	3	149.91	3.03	1.55E-02	1
3	474.55	34	12	8	9	2	100	3.24	1.17E-02	0

The predicted interaction of compounds (1–3) with cytochromes P450 isoform

Compound	GI absorption	BBB permeant	Pgp substrate	CYP1A2 inhibitor	CYP2C19 inhibitor	CYP2C9 inhibitor	CYP2D6 inhibitor	CYP3A4 inhibitor
1	High	No	Yes	No	No	No	Yes	No
2	Low	No	Yes	No	Yes	No	Yes	Yes
3	High	No	Yes	No	Yes	No	Yes	No

ProTox- II predicted organ toxicity, toxicological end points and acute toxicity

Compound	Hepatotoxicity	Neurotoxicity	Nephrotoxicity	Respiratory toxicity	Cardiotoxicity	Carcinogenicity	Immunotoxicity	Mutagenicity	Cytotoxicity	BBB-barrier
1	Inactive	Active	Inactive	Active	Inactive	Inactive	Active	Inactive	Inactive	Active
2	Inactive	Inactive	Active	Active	Inactive	Active	Active	Active	Inactive	Active
3	Inactive	Active	Active	Inactive	Inactive	Active	Active	Inactive	Active	Active

MW= Molecular weight; **NHA**=Number of ydrogen atoms; **NAHA**= Number of aromatic hetero atoms; **NRB**= Number of rotatable bonds; **NHBA** = Number of hydrogen acceptors; **NHBD**= Number of hydrgen donors.

Table 6
In-vitro DPPH radical scavanging activities of compounds **1**–**3**.

Conc. μg/ml	Comp 1		Comp 2		Comp 3		Ascorbic acid	
	% Inhibition	IC_{50}	% Inhibition	IC_{50}	% Inhibition	IC_{50}	% Inhibition	IC_{50}
2.5	12.675	37.802	15.015	30.392	17.015	72.2857	41.37	22.23
5	18.015		22.952		24.912		52.74	
10	24.952		30.033		29.029		62.33	
25	30.031		39.020		35.970		78.57	
50	36.970		47.563		42.021		98.79	
100	42.018		53.563		48.430		99.86	

Table 7
In-vitro anti-inflammatory activity of compound **1**–**3**.

Conc. μg/ml	% inhibition			
	Comp 1	Comp 2	Comp 3	Diclofenac sodium
2.5	17.53 ± 0.32	21.94 ± 0.76	8.76 ± 0.13	35.97 ± 0.22
5	18.78 ± 0.42	29.67 ± 0.49	11.52 ± 0.17	42.02 ± 0.64
10	22.54 ± 0.15	33.23 ± 0.38	19.29 ± 0.93	48.43 ± 0.79
25	29.43 ± 0.62	45.10 ± 0.27	25.57 ± 0.36	59.76 ± 0.86
50	33.65 ± 0.71	59.67 ± 0.45	30.68 ± 0.42	78.64 ± 0.92
100	43.50 ± 0.25	71.30 ± 0.37	39.30 ± 0.88	89.94 ± 0.39
Mean ± S.D; n = 3; p-value signifcant at $P < 0.001$				

Data availability

All the data is already included in main article and as supplementary material, the crsytal structure details on CCDC as RA2 (2178085) for compound 1 and RA2r (2178084) for compound 2.

CRediT authorship contribution statement

Rubina Siddiqui: Methodology, Investigation, Formal analysis, Data curation, Conceptualization. **Sana Shamim:** Writing – original draft, Project administration, Methodology, Formal analysis, Conceptualization. **Shamim Akhter:** Writing – review & editing, Supervision, Project administration, Conceptualization. **Samia Kausar:** Software, Methodology, Formal analysis. **Sammer Yousuf:** Software, Resources, Formal analysis, Data curation. **Ataf Ali Altaf:** Formal analysis, Data curation. **Zafar Saeed Saify:** Writing – review & editing, Validation, Supervision, Resources, Conceptualization. **Fuad Ameen:** Resources, Project administration, Funding acquisition.

Declaration of competing interest

The authors declare the following financial interests/personal relationships which may be considered as potential competing interests:Rubina Siddiqui reports financial support was provided by Higher Education Commission Pakistan. Fuad Ameen reports a relationship with King Saud University, Riyadh, Saudi Arabia. that includes: funding grants and non-financial support. Rubina siddiqui has patent pending to assignee. No such activity is related to the work If there are other authors, they declare that they have no known competing financial interests or personal relationships that could have appeared to influence the work reported in this paper.

Acknowledgments

The author thanks the Higher Education Commission (HEC) of Pakistan for their financial support in spectral data analysis.
This research was funded by Researchers Supporting Project number (RSP2024R364), King Saud University, Riyadh, Saudi Arabia.

Appendix A. Supplementary data

Supplementary data to this article can be found online at https://doi.org/10.1016/j.heliyon.2024.e35122.

References

[1] J. Dineshkumar, P. Parthiban, Synthesis, NMR study and antioxidant potency of 3, 5-dimethyl-2, 6-bis (2, 4-dichlorophenyl) piperidin-4-one, Res. J. Pharm. Technol. 15 (2022) 3641–3644, https://doi.org/10.52711/0974-360X.2022.00609.

[2] E.Y. Lim, C. Lee, Y.T. Kim, The antinociceptive potential of Camellia japonica leaf extract,(−)-epicatechin, and rutin against chronic constriction injury-induced neuropathic pain in rats, Antioxidants 11 (2022) 410, https://doi.org/10.3390/antiox11020410.

[3] P. Shukla, A. Asati, S.R. Bhardiya, M. Singh, V.K. Rai, A. Rai, Cu (I)-induced activation of furan for inverse electron demand ADAR with alkenes toward regioselective synthesis of tetrahydropyridine, J. Org. Chem. 85 (2020) 7772–7780, https://doi.org/10.1021/acs.joc.0c00279.

[4] S.K. Reshmi, E. Sathya, P.S. Devi, Isolation of piperdine from Piper nigrum and its antiproliferative activity, J. Med. Plants Res. 4 (2010) 1535–1546. DOI: 10.5897/JMPR10.033.

[5] S. Balasubramanian, C. Ramalingan, G. Aridoss, S. Kabilan, Synthesis and study of antibacterial and antifungal activities of novel 8-methyl-7, 9-diaryl-1, 2, 4, 8-tetraazaspiro [4.5] decan-3-thiones, Eur. J. Med. Chem. 40 (2005) 694–1546, https://doi.org/10.1016/j.ejmech.2005.02.001.

[6] A.K. Tripathi, A.K. Ray, S.K. Mishra, Molecular and Pharmacological Aspects of Piperine as a Potential Molecule for Disease Prevention and Management: Evidence from Clinical Trials, vol. 11, Beni-Suef university journal of basic and applied sciences, 2022, p. 16, https://doi.org/10.1186/s43088-022-00196-1.

[7] G. Pelletier, L. Constantineau-Forget, A.B. Charette, Directed functionalization of 1, 2-dihydropyridines: stereoselective synthesis of 2, 6-disubstituted piperidines, Chem. Commun. 50 (2014) 6883–6885, https://doi.org/10.1039/C4CC02220C.

[8] H.J. Hu, Q.Q. Wang, D.X. Wang, Y.F. Ao, Enantioselective biocatalytic desymmetrization for synthesis of enantiopure cis-3, 4-disubstituted pyrrolidines, Green Synthesis and Catalysis 2 (2021) 324–327, https://doi.org/10.1016/j.gresc.2021.07.002.

[9] C. Li, X. Zhou, F. Zhang, Z. Shen, Recent advances in the synthesis of nitrogen heterocycles using β-nitrostyrenes as substrates, Curr. Org. Chem. 27 (2023) 108–118, https://doi.org/10.2174/1385272827666230329104528.

[10] N. Nivetha, A. Thangamani, P.B. Raja, TiO2/SO4 2-solid superacid: a rapid, solventless, recoverable nanocatalyst for eco-friendly synthesis of piperidin-4-one oximes, Curr. Org. Chem. 27 (2023) 967–978, https://doi.org/10.2174/1385272827666230817144738.

[11] L. Nahakpam, M.D. Thiyam, W.S. Laitonjam, Simple and facile synthesis of 2-(arylamino)-1, 3-benzothiazoles using iodine–alumina (I2-Al2O3) as heterogenous catalyst and their antimicrobial activity, Russ. J. Org. Chem. 59 (2023) 133–141, https://doi.org/10.1134/S1070428023010141.

[12] Z.Y. Qi, S.Y. Hao, H.Z. Tian, H.L. Bian, L. Hui, S.W. Chen, Synthesis and biological evaluation of 1-(benzofuran-3-yl)-4-(3, 4, 5-trimethoxyphenyl)-1H-1, 2, 3-triazole derivatives as tubulin polymerization inhibitors, Bioorg. Chem. 94 (2020) 103392, https://doi.org/10.1016/j.bioorg.2019.103392.

[13] S. Shamim, H. Naseem, A. Saeed, S. Gul, S. Kosar, A.A. Altaf, F. Ameen, Synthesis, characterization, and antibacterial effectiveness of gemifloxacin C-3 modified amide analogs: a theoretical and experimental approach, J. Mol. Struct. (2024) 138573, https://doi.org/10.1016/j.molstruc.2024.138573.

[14] A.K. El-Damasy, H. Jin, M.A. Sabry, H.J. Kim, M.M. Alanazi, S.H. Seo, E.K. Bang, G. Keum, Design and synthesis of new 4-(3, 4, 5-trimethoxyphenyl) thiazole–pyrimidine derivatives as potential antiproliferative agents, Medicina 59 (2023) 1076, https://doi.org/10.3390/medicina59061076.

[15] N. Karaman, Y. Sıcak, T. Taşkın-Tok, M. Öztürk, A. Karaküçük-İyidoğan, Dikmen M, Koçyiğit-Kaymakçıoğlu B, Oruç-Emre EE. New piperidine-hydrazone derivatives: synthesis, biological evaluations and molecular docking studies as AChE and BChE inhibitors, Eur. J. Med. Chem. 124 (2016) 270–283, https://doi.org/10.1016/j.ejmech.2016.08.037.

[16] N.A. Frolov, A.N. Vereshchagin, Piperidine derivatives: recent advances in synthesis and pharmacological applications, Int. J. Mol. Sci. 24 (2023) 2937, https://doi.org/10.3390/ijms24032937.

[17] M. Budhiraja, A. Ali, V. Tyagi, First biocatalytic synthesis of piperidine derivatives via an immobilized lipase-catalyzed multicomponent reaction, New J. Chem. 46 (2022) 4837–4849, https://doi.org/10.1039/D1NJ06232H.

[18] M. Meenakumari, R. Girija, Molecular docking approach on potential of 2, 6-diphenylpiperidin-4-ol derivatives tfo inhibit covid 19 mainprotease, NVEO-NATURAL VOLATILES & ESSENTIAL OILS Journal| NVEO 10 (2023) 44–49, https://doi.org/10.53555/nveo.v10i1.4977.

[19] P. Asadi, M. Alvani, V. Hajhashemi, M. Rostami, G. Khodarahmi, Design, synthesis, biological evaluation, and molecular docking study on triazine based derivatives as anti-inflammatory agents, J. Mol. Struct. 1243 (2021) 130760, https://doi.org/10.1016/j.molstruc.2021.130760.

[20] A. Rodríguez, M.J. Romero, A. Fernández, M. López-Torres, D. Vázquez-García, L. Naya, J.M. Vila, J.J. Fernández, Dinuclear cyclometallated platinum (III) complexes. Relationship between molecular structure and crystal packing, Polyhedron 67 (2014) 160–170, https://doi.org/10.1107/S1600536811022744.

[21] K. Li, H. Zhang, C. Chang, K. Lin, B. Zhang, Z. Ma, D. Wei, Q. Zhang, A hydrogen bonded azine as a building block for π-conjugated polymers and their semiconducting properties, Polym. Chem. (2024), https://doi.org/10.1039/D3PY01346D.

[22] N.A. Frolov, A.N. Vereshchagin, Piperidine derivatives: recent advances in synthesis and pharmacological applications, Int. J. Mol. Sci. 24 (2023) 2937, https://doi.org/10.3390/ijms24032937.

[23] A. Ramalingam, Synthesis and crystallization procedure of piperidin-4-one and its derivatives: an update, Chemical Review and Letters 4 (2021) 192–199, https://doi.org/10.22034/CRL.2021.278234.1105.

[24] J. Jia, LaDuca RL. Poly [[μ-1, 4-bis (pyridin-4-ylmethyl) piperazine] bis [μ3-4-(2-carboxylatoethyl) benzoato] dicopper (II)], IUCrData (2023), https://doi.org/10.1107/S2414314623007459, 8:x230745.

[25] G. Ali, Understanding Dioxygen Activation Using Copper Complex, Doctoral dissertation, The University of Utah), 2021.

[26] O. Simsek, M. Ashfaq, M.N. Tahir, S. Ozturk, E. Agar, Synthesis and charaterizations of the Schiff base derived from 2-hydroxy-5-nitrobenzaldehyde alongwith Hirshfeld surface analysis and computational study, J. Struct. Chem. 64 (2023) 942–953, https://doi.org/10.1134/S0022476623050128.

[27] S. Yeşilbağ, S. Kansız, N. Dege, E. Ağar, Structural investigation and hirshfeld surface analysis of two [ONO]-Type schiff bases, J. Struct. Chem. 65 (2024) 464–477, https://doi.org/10.1134/S0022476624030041.

[28] E. Irrou, Y.A. Elmachkouri, A. Oubella, H. Ouchtak, S. Dalbouha, J.T. Mague, T. Hökelek, L. El Ghayati, N.K. Sebbar, M.L. Taha, Crystal structure determination, Hirshfeld surface, crystal void, intermolecular interaction energy analyses, as well as DFT and energy framework calculations of 2-(4-oxo-4, 5-dihydro-1H-pyrazolo [3, 4-d] pyrimidin-1-yl) acetic acid, Acta Crystallogr. E: Crystallographic Communications 78 (2022) 953–960, https://doi.org/10.1107/S2056989022008489.

[29] H.M. Imran, N. Rasool, I. Kanwal, M.A. Hashmi, A.A. Altaf, G. Ahmed, A. Malik, S. Kausar, S.U. Khan, A. Ahmad, S.A. Shah, Synthesis of halogenated [1, 1′-biphenyl]-4-yl benzoate and [1, 1′: 3′, 1 ″-terphenyl]-4′-yl benzoate by palladium catalyzed cascade C–C coupling and structural analysis through computational approach, J. Mol. Struct. 1222 (2020) 128839, https://doi.org/10.1016/j.molstruc.2020.128839doi.org/10.3390/molecules27123732.

[30] A. Daina, O. Michielin, V. Zoete SwissADME, A free web tool to evaluate pharmacokinetics, drug-likeness and medicinal chemistry friendliness of small molecules, Sci. Rep. 7 (2017) 42717, https://doi.org/10.1038/srep42717.

[31] Banerjee P., Kemmler E., Dunkel M., Preissner R.: ProTox 3.0: a Webserver for the Prediction of Toxicity of Chemicals Nucleic Acids Res (Webserver Issue 2024); NAR.

[32] I. Begum, S. Shamim, F. Ameen, Z. Hussain, S.A. Bhat, T. Qadri, M. Hussain, A combinatorial approach towards antibacterial and antioxidant activity using tartaric acid capped silver nanoparticles, Processes 10 (2022) 716, https://doi.org/10.3390/pr10040716.

[33] T. Fatima, H. Abrar, N. Jahan, S. Shamim, N. Ahmed, A.B. Ali, I. Begum, W. Ahmed, Molecular marker identification, antioxidant, antinociceptive, and anti-inflammatory responsiveness of malonic acid capped silver nanoparticle, Front. Pharmacol. 14 (2024) 1319613, https://doi.org/10.3389/fphar.2023.131961330.

[34] M.U. Khan, M. Khalid, R.A. Khera, M.N. Akhtar, A. Abbas, M.F. ur Rehman, A.A. Braga, M.M. Alam, M. Imran, Y. Wang, C. Lu, Influence of acceptor tethering on the performance of nonlinear optical properties for pyrene-based materials with A-π-D-π-D architecture, Arab. J. Chem. 15 (2022) 103673, https://doi.org/10.1039/D2RA01127A. **2022,** 15, 103673.

[35] M. Drissi, N. Benhalima, Y. Megrouss, R. Rachida, A. Chouaih, F. Hamzaoui, Theoretical and experimental electrostatic potential around the m-nitrophenol molecule, Molecules 20 (2015) 4042–4054, https://doi.org/10.3390/molecules20034042.

[36] V. Vidhya, A. Austine, M. Arivazhagan, Experimental approach, theoretical investigation and molecular docking of 2-chloro-5-fluoro phenol antibacterial compound, Heliyon 6 (2020) e05464, https://doi.org/10.1016/j.heliyon.2020.e05464.

[37] K. Nowosad, J. Bocianowski, F. Kianersi, A. Pour-Aboughadareh, Analysis of linkage on interaction of main aspects (genotype by environment interaction, stability and genetic parameters) of 1000 kernels in maize (Zea mays L.), Agriculture 13 (2023), https://doi.org/10.3390/agriculture13102005, 2005.
[38] Y. Wang, X. Wang, W. Zhang, W.H. Sun, Progress of ring-opening polymerization of cyclic esters catalyzed by iron compounds, Organometallics 42 (2023) 1680–1692, https://doi.org/10.1021/acs.organomet.3c00028.
[39] Quest Graph™ IC50 Calculator, AAT Bioquest, Inc. (2024). https://www.aatbio.com/tools/ic50-calculator.
[40] J. Chen, J. Yang, L. Ma, J. Li, N. Shahzad, C.K. Kim, Structure-antioxidant activity relationship of methoxy, phenolic hydroxyl, and carboxylic acid groups of phenolic acids, Sci. Rep. 10 (2020) 2611, https://doi.org/10.1038/s41598-020-59451-z.